Progress In Electromagnetics Research, PIER 72, 127–143, 2007

DESIGN AND ANALYSIS OF A LOW-FREQUENCY RADIO TELESCOPE FOR JOVIAN RADIO EMISSION

S. Joardar

Giant Meterwave Radio Telescope
Tata Institute of Fundamental Research
Khodad, Narayagaon, Pune-410504, Maharashtra, India

A. B. Bhattacharya

Department of Physics
University of Kalyani
Nadia-741235, West Bengal, India

Abstract—It is well known that planet Jupiter produces strong radio bursts at decametric wavelengths from regions of temporary radio emission in its magnetosphere. Like the man made radio signals, these signals do interfere in the low frequency radio telescope data while observing a different extraterrestrial source. Identification and characterization of this interfering signal is important in radio astronomy. In most of the radio astronomy sites, spectrum monitoring stations are available for such purposes. These instruments record any strong signal within the band and also aim to locate its position. Depending on the properties of different categories of sources, special modules can be attached to these instruments for obtaining a more detailed picture. These modules can be added at the front end of the instrument using a selector switch and can be connected whenever necessary. Construction of one such module for capturing and recording the Jupiter radio bursts has been described with all the engineering details. It consists of an antenna system followed a receiver (connected to a spectrum recorder). An improvement in the antenna system has been made as compared to the contemporarily available single antenna Jupiter radio telescopes, thereby enabling to record the radio emissions over a larger period using a fixed beam. The receiver system has been designed to process the low frequency Jovian signals from 18 to 25 MHz. The back end is that of a spectrum monitoring system which serves as an automated data analyzer and

recorder. It offers flexibility and various setup choices to the user. The mathematical analysis of the instrument and computed system characteristics have been produced in detail for ease of reproductions, direct use in radio astronomy and future design developments.

1. INTRODUCTION

The spectrum monitoring stations [1, 2] for assisting radio astronomy can also be used for capturing the Jupiter and solar radio bursts. At times, the RFI[†] could be of extraterrestrial origin but may appear to have generated from ordinary electrical disturbance produced out of randomly fluctuating currents and can be confusing to the observer. In order to categorize the origin of the signal, viz. terrestrial (local) or extraterrestrial, it is advantageous to have additional modules which could be switched into under such situations. Additionally, the spectrum monitoring stations could also be used as detector for radio-transients and glowing radio sources in astronomy. Two well known strong radio burst generators within our solar system are the Sun and the planet Jupiter. Here we shall discuss only the module designed especially for Jovian decametric radio emission.

The planet Jupiter significantly emits radio signals from just below 40 MHz down to a few kilohertz, though higher frequency emission may also exist. In 1955 the Jovian decameter wavelength emission at the 22.2 MHz was discovered by Burke and Franklin [3]. In 1956 Kraus reported the distinctive short staccato bursts (from Jupiter) [4]. Today it is understood that there are different sources emitting radio emissions from the magnetosphere of Jupiter [5]. The probability of these radio emissions is strong when (i) certain longitudes of Jupiter labeled A, B and C face the Earth, and or (ii) certain combinations of Jupiter's central meridian longitude (CML) with the position of the Jovian moon Io in its orbit around the planet [6]. The easily detectable radio noise storms occur just above 15 MHz up to a practical limit of about 38 MHz. The Earth's ionosphere severely attenuates or refracts away extraterrestrial signals below 15 MHz. Chances of interference from radio broadcasting stations upto 18 MHz are reasonably high. As the upper limit is reached, the strength of the signals is found to diminish rapidly. The Solar activity nearing its peak in every 11 years can keep the ionosphere excited [7]. Thus the distinct range of picking the Jupiter's signals would be 18 to 25 MHz. Hence constructions of radio telescopes for Jupiter are optimized towards this

[†] Any man made or unidentified signal interfering with the desired extraterrestrial signal is termed as 'RFI' or radio frequency interference.

range of frequency. This non-thermal emission from the Jupiter is very intense with effective source temperature lying between 10^{15} to 10^{20} K, circularly or elliptically polarized and the instantaneous size of the emission regions are usually much less than 400 km [8].

Till now many instruments for detecting the radio bursts from Jupiter, similar to that of NASA's Radio Jove project[‡], have been replicated all over the world. They record the data digitally using a sound card and are usually narrow band. These systems are generally single antenna type consisting of a thin (narrow band) dipole. Some available systems use portable antennas and are positioned manually depending on the Jupiter's position on the sky. For any scientific purpose, the instruments used need to be thoroughly calibrated with the position of the source in sky. The calibration changes if the antenna position is changed within the coordinate system used. However, if the antenna is rigid, a single time calibration could serve over a long period of time. In this article we describe an instrument possessing a rigid antenna system, especially designed for equatorial and tropical regions. The effect of the ground [9] has been engineered using an additional reflector[§] to produce an uniform illumination of the Jovian path in the sky under a single major lobe. It is advantageous to increase the conductivity of the ground by spreading metallic mesh over it within a circle of 250 m radius. A cylindrical dipole (sometimes called a fat dipole) is designed for obtaining increased bandwidth. The back-end of the system is a spectrum analyzer connected to a computer with data collecting interface. This part commonly exists in most of the spectrum monitoring systems and offers the user a much larger selectable bandwidth and more flexibility in system settings. The design details of the antenna system are produced under Section 2. In Section 3, the receiver system design has been covered followed by its analysis in Section 4. The results of analysis are presented in Section 5, and finally the discussions and conclusions are presented in Section 6.

2. ANTENNA SYSTEM

Ideally, the antenna beamwidths of a radio telescope should be equal or less than the extents of the extraterrestrial radio source and should be kept pointed towards the source throughout the period of observation such that only the signals from the source are picked up and not the noise from the background (sky). This is extremely important

[‡] See their website http://radiojove.gsfc.nasa.gov.

[§] Its design has been perfected with lots of trial and error. Throughout this article we shall address it as 'special reflector'.

for weak radio sources which are only a few times stronger than the background radiation from the sky. But the Solar and Jovian radio bursts are strongest (on Earth) among all the extraterrestrial signals known today and their flux densities are comparable to those produced by communication transmitters. Hence a wide beam antenna can be used. Most of the extraterrestrial objects as seen from the Earth's equator rise from the eastern horizon and set in the western horizon. However, if the observation is made from regions above or below the equator, the objects will be seen to trace their paths within the northern or southern hemisphere of the sky respectively. Thus for tropical and equatorial regions, the antenna employed for the Jupiter should have a uniform coverage of the sky from east to west extending about 80° across at the zenith. In other words, the radiation pattern should uniformly illuminate a certain solid angle lying between the northern and southern sky and stretched between east and west such that signals from the object are not missed out. The situation is shown in Fig. 1. The gray colored belt contains the astronomical object within it. Note that the belt is wider around the zenith and narrower on the horizon ($\delta > \delta'$). In order to receive signals from a source moving on this belt, one requires an antenna focused towards the zenith, whose beam pattern's cross section should be an ellipse having its major axis along east-west and minor axis along north-south directions. If the half power beamwidths in the north-south-zenith plane and in the east-west-zenith plane are δ and α respectively, then depending on the value of α the maximum period of observation is determined, and the value of δ provides a measure for determining the minimum and maximum latitude coverage on Earth. Since the bandwidth of observation is nearly 32% (18–25 MHz), a single cylindrical dipole [10] antenna, positioned above the ground along the north-south works satisfactorily. A folded dipole is preferred for it has a simple balun matching.

Positioning an antenna above the ground is likely to change its radiation pattern, since the later substantially reflects the electromagnetic waves [9]. Depending on the distance between the ground and the antenna, changes in the phases of the signals reaching the antenna by reflection take place. These result in constructive, destructive, semi-constructive or semi-destructive interferences between the direct signals and the reflected signals reaching the antenna. Hence the pattern of the antenna completely changes from what it would be if the antenna was placed in a free space. In the present design, the reduction in the antenna gain towards the zenith due to ground reflection has been compensated by the special reflector positioned between the antenna and ground. The position of

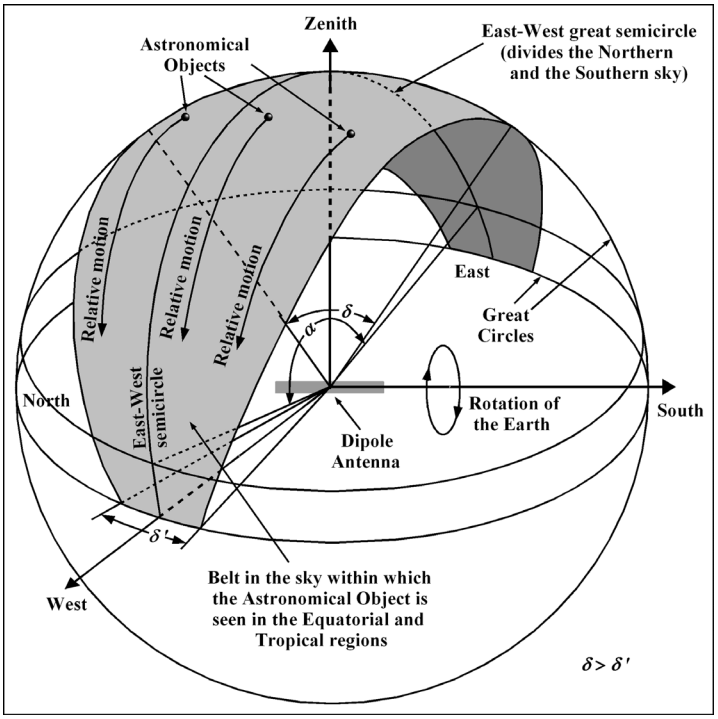

Figure 1. Motion of the astronomical objects as observed from the equatorial and tropical regions on Earth. The extents of the half power antenna beamwidths are indicated by α and δ.

the reflector with respect to the ground and the dipole, and its size are critical. Changing any of these by about 10% of the wavelength would result in a different antenna pattern. The dimensions are finalized purely on trial and error basis after having simulated several structures using method of moments. Figs. 2(a) and 2(b) show the details of the antenna system design. Fig. 2(c) shows the details of the dipole design. The dipole has been designed using aluminum tubes of different diameters with a natural balun [11] which directly gives a coaxial output. The outer shielding of the coaxial cable is connected to the special reflector and to the ground. Following this, it is fed to the BPF[‖] followed by rest of the system. Effectively, the antenna system produces a single beam pattern illuminating the major portion of the observation belt (explained earlier in Fig. 1). The antenna (thermal) efficiency ε_{Ant} [11] can be safely taken as 90%.

[‖] A 'BPF' or band pass filter is used to eliminate the spectrum outside the required range.

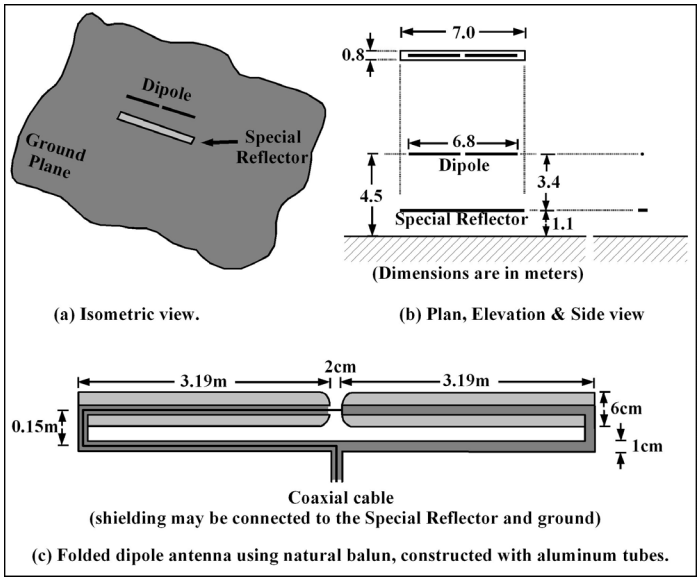

Figure 2. Details of the antenna system. (a) Isometric view. (b) Plan, elevation and side view. (c) Details of the 20 MHz cylindrical folded dipole antenna with balun.

Due to the practical limitations as a result of the large rigid structure of the antenna system, it is not possible to measure radiation patterns with the ground included with conventional methods using any artificial RF-source. In our experience we felt that simulations may provide a closely approximate picture. The simulations were done using some MATLAB based software tools [12]. The radiation patterns are shown in Fig. 3 with respect to the position of the dipole axis (lying above the ground and the reflector). With a minimum gain of 3 dBi, the east-west coverage angle α is approximately 120° while the north-south coverage angle δ is round about 90° throughout the entire frequency band of observation. The values of α and δ are also approximate mean of the half power beamwidths (all frequency patterns). In a horizon system of coordinates [13], the Jupiter can be safely observed from tropical or equatorial regions, if the former posses an altitude greater than 30° and azimuth between 50° and 130° or between 230° and 310°. In other words, the radio observations can be continued for 8 hours, starting with the Jupiter's position 30° above the eastern horizon and ending with the Jupiter reaching a point 30° above the western horizon provided it stays within ±40° from the line separating the northern and the southern sky.

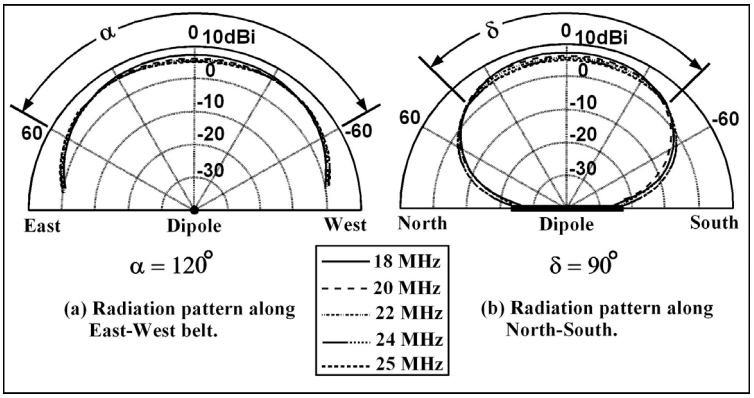

Figure 3. Simulated radiation patterns of the dipole kept above the special reflector as shown in Fig. 2. As can be seen from the patterns, the east-west coverage is about 150° and the north-south belt coverage is about 90° (at zenith) for the observation frequency range of 18 to 25 MHz.

3. CONSTRUCTIONAL DETAILS OF THE RECEIVER SYSTEM

For observing the radio bursts from the Jupiter, using the simplest form of instrumental setup, one needs an antenna, and a spectrum analyzer. However, if the distance between the antenna and the spectrum analyzer is large, one might incorporate a BPF at the antenna output followed by an LNA¶. The purpose of inserting the BPF before the LNA is to avoid any out of band RFI like commercial shortwave broadcasting channels, which could otherwise be substantially powerful in driving the LNA into nonlinearity or saturation. These could lead to the generation of inter-modulation products within the working band. Fig. 4 shows the complete instrumentation block diagram. There are several front end modules selectable by the RF-switch. The back end of the system is common to all the modules which contain the data recording arrangement. The spectrum analyzer is interfaced with a computer for (a) remotely setting it and (b) for continuous data recording.

The BPF has been constructed using lumped electronic components. The design is a 7^{th} order chebyshev with 0.5 dB pass band ripple and average insertion loss of 0.24 dB across the band. It

¶ An 'LNA' or low noise amplifier is connected close to the antenna to boost the signals with least deterioration of the signal to noise ratio.

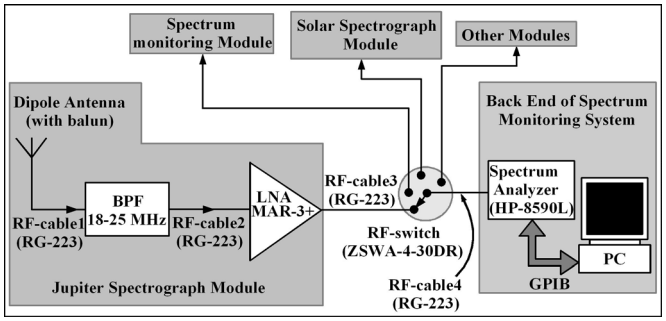

Figure 4. System block diagram of the Jupiter's decametric radio burst recorder (Jupiter Spectrograph Module) connected with the back end of a spectrum monitoring system using a RF-switch.

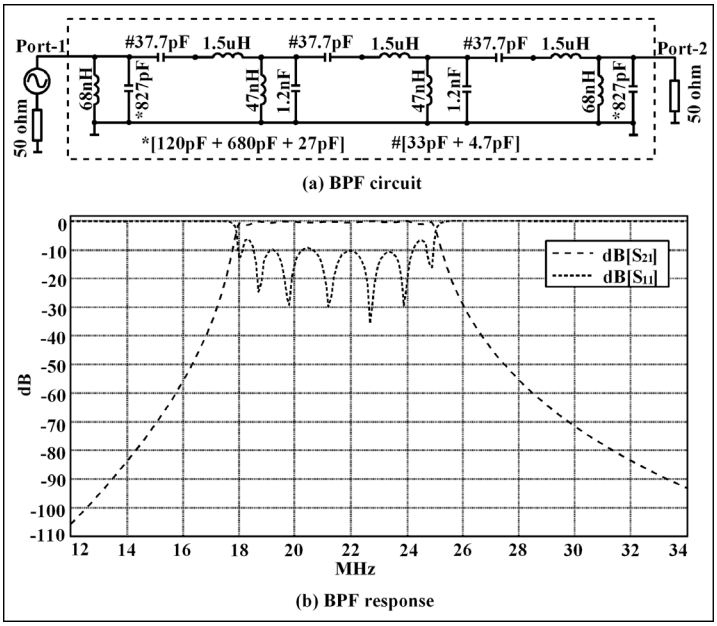

Figure 5. Details of the 18–25 MHz bandpass filter. (a) Circuit diagram. (b) S-parameter response in dB. The return loss (at port-1) and the transmission characteristics are shown.

is preferable to fabricate it on a glass epoxy double layer PCB based on microstrip structure with 50 ohm SMA connectors at the input and output ports (ports 1 and 2). The detailed circuit diagram and S-parameter response are shown in Fig. 5.

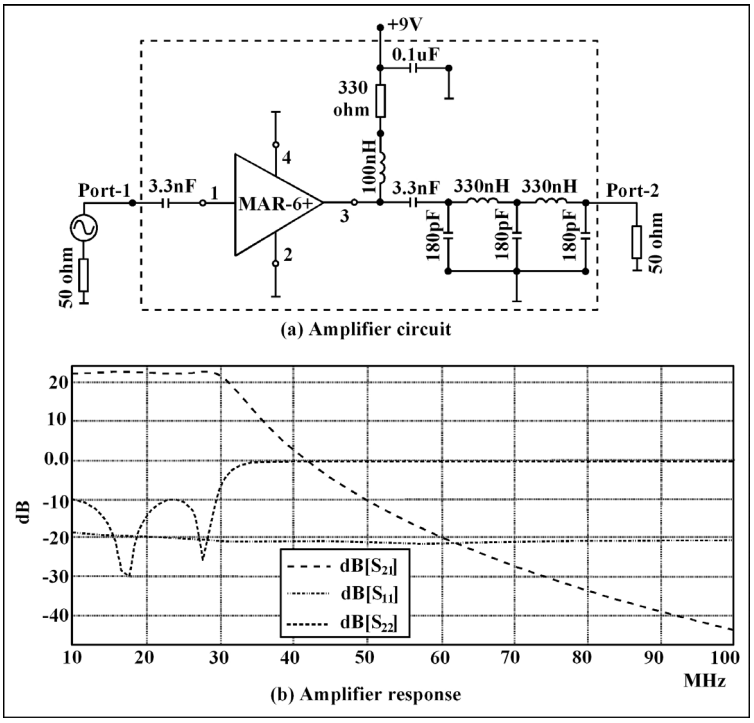

Figure 6. Details of the amplifier design. (a) Circuit diagram. (b) S-parameter response in dB.

The LNA has been constructed using a monolithic microwave amplifier chip from MiniCircuits. It has a typical gain of 22 dB, a specified noise figure of 3 dB and the 1 dB gain compression at 3 dBm power output. Fig. 6 shows the design and response of the amplifier. A low pass filter circuit has been inserted after the amplifier module to limit the usable bandwidth to 30 MHz. It is preferable to fabricate it on a double layer PCB based on microstrip structure with 50 ohm SMA connectors for the input and output ports (ports 1 and 2). It has been designed for a bias voltage of +9 volts so that it could also be battery operated. Different lengths of the cables are employed at different places which introduce different amount of attenuations. The 8590L spectrum analyzer from HP-Agilent has been used. In our calculations, we have chosen the resolution bandwidth $\Delta\nu_{res}$ and video bandwidth $\Delta\nu_{vid}$ as 1 kHz though not a mandatory choice. For data recording, a GPIB[+] interface has been used between the computer and

[+] 'General Purpose Interface Bus', also known as HPIB, named by its inventor company

the spectrum analyzer. The user sets spectrum analyzer with desired specifications using a GUI based software available on the computer. Additionally, the starting time and the duration of observation are also set. Table 1 lists the values of the different parameters of the instruments, objects and devices used. The symbol ε with any subscript has been used to represent the transmission characteristics of passive devices.

Table 1. Used parameters of the devices, objects and instruments used.

Device/Object	Name / Make / Settings / Parameters
Antenna with Special Reflector	Min. gain $G_{Ant} = 2$ (3 dBi), Frequency Range: 18–25 MHz $\varepsilon_{Ant} = 0.9$, Mean half power beamwidths: $\alpha = 120^\circ, \delta = 90^\circ$
Low Noise Amplifier	MAR-6 [monolithic amplifier chip from MiniCircuits] Noise figure $NF_{LNA} = 2$ (3 dB), $G_{LNA} = 158.48$ (22 dB)
Spectrum Analyzer	HP-8590L, $\Delta\nu_{res} = \Delta\nu_{vid} = 1$ kHz, $FreqSpan = 7$ MHz $NoiseFloor = 10^{-11}$ mW (-110 dBm), $SweepTime = 21$ sec.
RF-Cable-1	RG-223 (11 m), $\varepsilon_{cable1} = 0.87$ (Insertion loss = 0.605 dB)
RF-Cable-2	RG-223 (0.5 m), $\varepsilon_{cable2} = 0.99$ (Insertion loss = 0.028 dB)
RF-Cable-3	RG-223 (50 m), $\varepsilon_{cable3} = 0.53$ (Insertion loss = 2.75 dB)
RF-Cable-4	RG-223 (0.5 m), $\varepsilon_{cable4} = 0.99$ (Insertion loss = 0.028 dB)
RF-switch	ZSWA-4-30DR [MiniCircuits] $\varepsilon_{RFswitch} = 0.79$ (Insertion loss = 1.0 dB)
Radio Jupiter	Min. Flux density at antenna aperture $S_{radioSrc} = 10^{-22}$w/m^2/Hz

4. ANALYSIS OF THE RECEIVER SYSTEM

The analysis is similar to that of any radio receiving system used for radio astronomy [1] and RADAR applications [14]. The equations derived are applicable within 18–25 MHz where the filters operate within their pass-bands. As shown in the system block diagram in Fig. 4, the signals collected from the antennas are filtered, amplified and fed to a spectrum analyzer. Depending on the strength of the amplified signal, the resolution bandwidth $\Delta\nu_{res}$ and the

Hewlet Packart (HP or HP-Agilent).

video bandwidth $\Delta\nu_{vid}$ of the spectrum analyzer are set. The number of spectral channels within a spectrum trace is expressed in equation (1) [15]. The noise temperature of the spectrum analyzer $T_{specAna}$ is expressed in equation (2) [1], where $T_{specAnaPhy}$ is its physical temperature. Here onwards any subscript (used along with any variable) ending with *phy* or *Phy* shall indicate its physical temperature. Similarly, any subscript ending with *sys* or *Sys* shall indicate its contribution to the system temperature. The integration time of the spectrum analyzer for each sweep is expressed in equation (3) [15]. The temperature contribution of the spectrum analyzer $T_{specAnaSys}$ towards the system temperature is expressed in equation (4), where, G_{LNA} is the linear gain of the LNA, and the symbol ε with any subscript name represents the output to input power ratio of that passive device. The contribution to the system temperatures from the RF-cables, LNA and RF-switch are expressed in equations (5) through (11), where NF_{LNA} is the linear noise figure of the LNA. The antenna's contribution to system temperature is expressed in equation (12), where ε_{Ant} is the antenna (thermal) efficiency [11], T_{sky} is the temperature of the sky and T_{gnd} is the tmperature of the ground (approximately 5% of the antenna patterns appear as back lobes). The overall system temperature is expressed in equation (13). The effective integration time can be expressed as in equation (14) where, N_{sweep} is the total number of video averages including post-video-averages* [1]. The minimum detectable temperature ΔT_{min} of the system is expressed in equation (15). If $S_{radioSrc}$ is the radio flux density in $\mathrm{wm^{-2}Hz^{-1}}$ produced by the Jupiter at the surface of the antenna, the signal to noise ratio SNR of the system can be expressed as in equation (16), where k is the Boltzmann constant G_{Ant} is the linear gain of the antenna, λ_{sig} is the wavelength of the signal and $\Delta\nu_{sig}$ is its bandwidth.

$$\text{No. of Spectral Channels} = \left(\frac{\text{Frequency Span}}{\Delta\nu_{res}}\right) \tag{1}$$

$$T_{specAna} = \left(\frac{NoiseFloor}{k\ \Delta\nu_{res}} - T_{specAnaPhy}\right) \tag{2}$$

$$\tau = \left(\frac{1}{2\ \Delta\nu_{vid}}\right) \tag{3}$$

* Here we restrict the number of sweeps to unity since we are interested in the shape of radio bursts. Increasing the number of averages more than one will destroy the signature and shape of the bursts. However, it may be used for special purposes like mean power analysis.

$$T_{specAnaSys} = \left(\frac{T_{specAna}}{G_{LNA}\ \varepsilon_{cable1}\ \varepsilon_{cable2}\ \varepsilon_{cable3}\ \varepsilon_{cable4}\ \varepsilon_{BPF}\ \varepsilon_{RFswitch}}\right) \tag{4}$$

$$T_{cable1Sys} = T_{cable1Phy}\left(\frac{1}{\varepsilon_{cable1}} - 1\right) \tag{5}$$

$$T_{BPFsys} = \left(\frac{T_{BPFphy}}{\varepsilon_{cable1}}\right)\left(\frac{1}{\varepsilon_{BPF}} - 1\right) \tag{6}$$

$$T_{cable2Sys} = \left(\frac{T_{cable2Phy}}{\varepsilon_{BPF}\,\varepsilon_{cable1}}\right)\left(\frac{1}{\varepsilon_{cable2}} - 1\right) \tag{7}$$

$$T_{LNAsys} = \left(\frac{T_{LNAphy}\,(NF_{LNA} - 1)}{\varepsilon_{cable1}\varepsilon_{BPF}\varepsilon_{cable2}}\right) \tag{8}$$

$$T_{cable3Sys} = \left(\frac{T_{cable3Phy}}{G_{LNA}\varepsilon_{BPF}\varepsilon_{cable1}\varepsilon_{cable2}}\right)\left(\frac{1}{\varepsilon_{cable3}} - 1\right) \tag{9}$$

$$T_{RFswitchSys} = \left(\frac{T_{RFswitchPhy}}{G_{LNA}\varepsilon_{BPF}\varepsilon_{cable1}\varepsilon_{cable2}\varepsilon_{cable3}}\right)\left(\frac{1}{\varepsilon_{RFswitch}} - 1\right) \tag{10}$$

$$T_{cable4Sys} = \left(\frac{T_{cable4Phy}}{G_{LNA}\varepsilon_{BPF}\varepsilon_{cable1}\varepsilon_{cable2}\varepsilon_{cable3}\varepsilon_{RFswitch}}\right)\left(\frac{1}{\varepsilon_{cable4}} - 1\right) \tag{11}$$

$$T_{AntSys} = 0.95T_{sky} + T_{AntPhy}\left(\frac{1}{\varepsilon_{Ant}} - 1\right) + 0.05T_{gnd} \tag{12}$$

$$\begin{aligned} T_{sys} = {} & T_{AntSys} + T_{LNAsys} + T_{specAnaSys} + T_{cable1Sys} + T_{cable2Sys} \\ & + T_{cable3Sys} + T_{BPFsys} + T_{RFswitchSys} + T_{cable4Sys} \end{aligned} \tag{13}$$

$$\begin{aligned} & \tau_{eff} = (N_{sweep}\tau)\,, \quad N_{sweep} = 1, 2, 3... \\ & \text{where, } \tau = \frac{\text{Sweep Time}}{\text{No. of Spectral Channels}} \end{aligned} \tag{14}$$

$$\Delta T_{\min} = \left(\frac{T_{sys}}{\sqrt{\tau_{eff}\,\Delta\nu_{res}}}\right)$$

$$\text{for burst detection, } \tau_{eff} = \tau, \text{ since } N_{sweep} = 1 \tag{15}$$

$$SNR = \left(\frac{S_{radioSrc}\,G_{Ant}\,\lambda_{sig}^2\sqrt{N_{sweep}}\,\Delta\nu_{sig}}{4\,\pi\,k\,T_{sys}\sqrt{2\,\Delta\nu_{res}\,\Delta\nu_{vid}}}\right), \quad \Delta\nu_{res} \le \Delta\nu_{sig}$$

$$\text{for burst detection, } N_{sweep} = 1 \tag{16}$$

5. RESULTS OF ANALYSIS

The antenna off-source temperatures at various frequencies are calculated based on the distribution of antenna beam over different regions of the sky and the ground. The sky noise temperature varies with frequency [11] and is near about 17,000 K at 22 MHz except on the galactic plane where it is very high [16]. Fig. 7 shows a sky map broadly dividing it into two temperature regions using galactic coordinates. The temperature of the sky could vary from 20,000 to 250,000 K within the gray belt extending from 0° to 360° in longitude and −20° to +20° in latitude. The mean temperature of this belt may be roughly estimated as 100,000 K. The equatorial coordinates projected on the map indicate the timings during which a pencil beam antenna pointed towards the zenith would pick up the galactic plane's temperature. For the current system, the antenna beam extends 120° in the east-west direction at the equator which is three times of the shown galactic plane's high temperature region. Physical temperature of the system is assumed to be 300 K. The system temperatures and

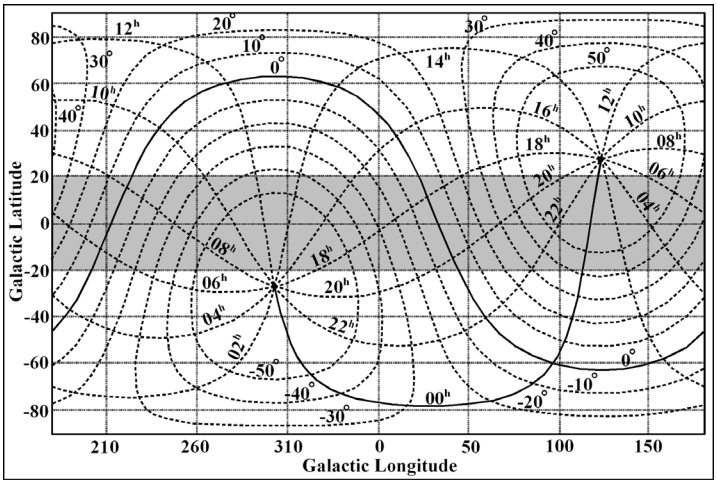

Figure 7. The sky has been roughly divided into high and low temperature regions in galactic coordinate system. The gray belt within ±20° latitudes, covering 360° in longitude contains the galactic plane, where the temperature could vary between 20,000 K and 250,000 K at 22 MHz. Major portion of rest of the sky is below 20,000 K. Equatorial coordinates are projected on the map to visualize the interaction timings of the high temperature region on the antenna system.

the minimum detectable temperatures are calculated for two cases, viz. with and without contribution from galactic plane. The signal to noise ratio have been calculated for a Jupiter signal of 1 SFU[♯] assuming the signal bandwidth as 7 MHz. Tables 2 and 3 display the results of analysis respectively with and without galactic plane's contribution. A typical radio burst captured using the instrument has been theoretically calibrated and presented in Fig. 8.

Table 2. System Characteristics for $\Delta\nu_{res} = 1\,\text{kHz}$, $\Delta\nu_{vid} = 1\,\text{kHz}$, $\tau = 0.0525\,\text{s}$ (inclusive of the radio contribution from Galactic plane).

Freq. (MHz)	18	19	20	21	22	23	24	25
T_{AntSys} ($\times 10^4\,^\circ$K)	4.36	4.29	4.22	4.15	4.08	4.01	3.94	3.87
T_{sys} ($\times 10^4\,^\circ$K)	5.75	5.68	5.61	5.54	5.47	5.40	5.33	5.26
ΔT_{min} ($\times 10^4\,^\circ$K) for $N_{sweep} = 1$	3.32	3.28	3.24	3.20	3.16	3.12	3.09	3.04
SNR (dB) at 1 SFU,$\Delta\nu_{sig} = 1\,\text{MHz}$	14.4	14.0	13.6	13.2	12.9	12.5	12.2	11.9

Table 3. System Characteristics for $\Delta\nu_{res} = 1\,\text{kHz}$, $\Delta\nu_{vid} = 1\,\text{kHz}$, $\tau = 0.0525\,\text{s}$ (exclusive of the radio contribution from Galactic plane).

Freq. (MHz)	18	19	20	21	22	23	24	25
T_{AntSys} ($\times 10^4\,^\circ$K)	1.82	1.72	1.62	1.52	1.41	1.31	1.20	1.09
T_{sys} ($\times 10^4\,^\circ$K)	3.22	3.11	3.01	2.91	2.80	2.70	2.59	2.49
ΔT_{min} ($\times 10^4\,^\circ$K) for $N_{sweep} = 1$	1.86	1.80	1.74	1.68	1.62	1.56	1.50	1.44
SNR (dB) at 1 SFU,$\Delta\nu_{sig} = 7\,\text{MHz}$	16.9	16.6	16.3	16.0	15.9	15.6	15.4	15.2

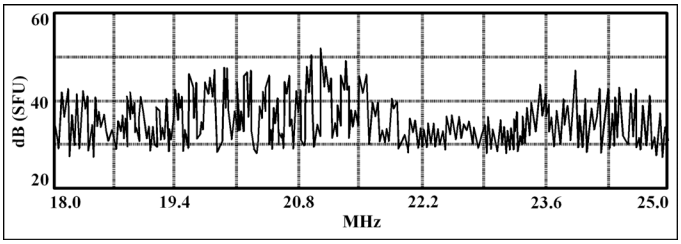

Figure 8. A typical radio burst captured using the present instrument and calibrated theoretically.

[♯] Solar flux unit. 1 SFU = 10^{-22} wm^{-2}Hz^{-1}

6. DISCUSSIONS AND CONCLUSIONS

Though problems from radio interferences are minimum at radio telescope sites, it is likely that some interference may be produced by the sky wave transmitters. These may be identified in the data as fixed frequency stationary/long-duration narrow band lines and may be removed [2]. As mentioned earlier in Section 2, the calibration of the antenna could be difficult since it requires a strong source to move across the antenna illumination pattern. Indirect calibration could be a possibility. This may be done by comparing the data obtained from the Solar or Jupiter bursts simultaneously taken from a calibrated radio telescope operating in the same frequency band. The position of the source can be calculated astronomically with respect to each of the two instruments. However, completing this process of calibration might take a much longer duration. The theoretical estimations presented in Tables 2 and 3 may be used temporarily till the calibration procedure is complete. To compensate for the variations introduced by the electronics (excluding the antenna), the antenna system may be disconnected from time to time within the observation and replaced by a calibrated noise source. An electronic arrangement could be made for this purpose using a SPDT RF-switch between the antenna/noise-source and the receiver. Since the beam pattern is extremely broad, it is possible that a Solar burst may interfere with that of the Jupiters, if observation is during day time. It may be preferred to observe the Jupiter during the night, especially during the periods of Solar activity. Since in general, the Jovian decametric radio bursts are elliptically polarized, the effect of Faraday rotation while passing through the ionosphere can significantly alter this information. Studying these phenomena is out of the scope of the present instrument, since it uses a single linearly polarized antenna. However it can be used for studying the variation of frequency and power with time which also is of significant scientific importance.

In this article we have shown the engineering details and analysis of a Jovian decameter wavelength radio burst capturing module for use at equatorial and tropical locations. The system can be an integrated part of any spectrum monitoring station assisting radio astronomy. Improvement in the antenna system has been made with a specially designed reflector. The bandwidth reasonably covers the transparent portion of the low frequency Jovian radio window available on Earth. The system is flexible and offers various setup choices to the user with automatic data recording. A detailed documentation has been presented here with the objective that any radio engineering/astronomy center or university should easily be able

to construct, calibrate and analyze the data obtained for the purpose of instrumentation and radio astronomy.

ACKNOWLEDGMENT

We are thankful to the reviewers and Ananda Hota for their valuable comments and suggestions. We acknowledge the Tata Institute of Fundamental Research and the University of Kalyani for their interest and support towards this work. Finally we acknowledge the Gmsh software group for having used their free software tools on finite element modeling and mesh generation.

REFERENCES

1. Joardar, S. and A. B. Bhattacharya, "Simultaneous resolving of frequency separated narrow band terrestrial radio sources by multi antenna spectrum monitoring systems assisting radio astronomy," *Journal of Electromagnetic Waves and Applications*, Vol. 20, No. 9, 1195–1209, 2006.
2. Joardar, S. and A. B. Bhattacharya, "Algorithms for categoric analysis of interference in low frequency radio astronomy," *Journal of Electromagn. Waves and Applications*, Vol. 21, No. 4, 441–456, 2007.
3. Burke, B. F. and K. L. Franklin, "Observations of a variable radio source associated with the planet Jupiter," *Journal of Geophysical Research*, Vol. 60, 213, 1955.
4. Kraus, J. D., "Planetary and solar radio emission at 11 meters wavelength," *Proceedings of the IRE*, Vol. 46, Issue 1, 266–274, 1958.
5. Lecacheux, A., M. Y. Boudjada, H. O. Rucker, J. L. Bougeret, R. Manning, and M. L. Kaiser, "Jovian decametric emissions observed by the Wind/WAVES radioastronomy experiment," *Astronomy and Astrophysics*, Vol. 329, 776–784, 1998.
6. Oueinnec, J. and P. Zarka, "Io-controlled decameter arcs and Io-Jupiter interaction," *Journal of Geophysical Research*, Vol. 103, 26649–26666, 1998.
7. Anastassiades, M., D. Ilias, and E. Tsagakis, "On ionospheric disturbances caused by the solar activity of November 1960," *Pure and Applied Geophysics*, Vol. 51, No. 1, 142–146, 1962.
8. Zarka, P., "Fast radio imaging of Jupiter's magnetosphere at low-frequencies with LOFAR," *Planetary and Space Science*, Vol. 52, 1455–1467, 2004.

9. Uduwawala, D., M. Norgren, and P. Fuks, "A complete FDTD simulation of a real GPR antenna system operating above lossy and dispersive grounds," *Progress In Electromagnetics Research*, PIER 50, 209–229, 2005.
10. Papakanellos, P. J., I. I. Heretakis, P. K. Varlamos, and C. N. Capsalis, "A combined method of auxiliary sources-reaction matching approach for analyzing moderately large-scale arrays of cylindrical dipoles," *Progress In Electromagnetics Research*, PIER 59, 51–67, 2006.
11. Kraus, J. D., R. J. Marhefka, et al., *Antennas for All Applications*, Tata McGraw-Hill, New Delhi, 2003.
12. Makarov, S. N., *Antennas and EM modeling with MATLAB*, John Willy and Sons, New York, 2002.
13. Birney, D. S., *Observational Astronomy*, Cambridge University Press, Cambridge, 1991.
14. Chan, Y. K., B. K. Chung, and H. T. Chuah, "Transmitter and receiver design of an experimental airborne synthetic aperture RADAR sensor," *Progress In Electromagnetics Research*, PIER 49, 203–218, 2004.
15. Packard, H., *Spectrum Analysis: Application Note 150*, Hewlet Packard Company, California, 1989.
16. Roger, R. S., C. H. Costain, T. L. Landecker, and C. M. Swerdlyk, "The radio emission from the Galaxy," *Astronomy and Astrophysics Supplement Series*, Ser. 137, 7–19, 1999.